



1 **Investigating the impact of regional transport on PM_{2.5}**
2 **formation using vertical observation during APEC 2014**
3 **Summit in Beijing**

4 Yang Hua^{1,2}, Shuxiao Wang^{1,2*}, Jiandong Wang^{1,2}, Jingkun Jiang^{1,2}, Tianshu Zhang³,
5 Yu Song⁴, Ling Kang⁴, Wei Zhou^{1,2}, Runlong Cai^{1,2}, Di Wu^{1,2}, Siwei Fan^{1,2}, Tong
6 Wang^{1,2}, Xiaoqing Tang⁵, Qiang Wei⁶, Feng Sun⁶, Zhimei Xiao⁷

7 ¹State Key Joint Laboratory of Environment Simulation and Pollution Control, School of
8 Environment, Tsinghua University, Beijing 100084, China.

9 ²State Environmental Protection Key Laboratory of Sources and Control of Air Pollution Complex,
10 Beijing 100084, China

11 ³Anhui Institute of Optics and Fine Mechanics, Chinese Academy of Sciences, Hefei 230031, China

12 ⁴College of Environmental Sciences and Engineering, Peking University, Beijing, 100871, China

13 ⁵Hebei Environmental Monitoring Center, Hebei 050051, China

14 ⁶Beijing Environmental Monitoring Center, Beijing 100048, China

15 ⁷Tianjin Environmental Monitoring Center, Tianjin 300191, China

16 Corresponding to: Shuxiao Wang (shxwang@tsinghua.edu.cn)

17 **ABSTRACT**

18 During APEC (Asia-Pacific Economic Cooperation) Economic Leaders' 2014 Summit in Beijing,
19 strict regional air emission control was implemented, providing a unique opportunity to investigate
20 the transport and formation mechanism of fine particulate matter (PM_{2.5}). This study explores the use
21 of vertical observation methods to investigate the influence of regional transport on PM_{2.5} pollution in
22 Beijing before and during the APEC Summit. Vertical profiles of extinction coefficient, wind,
23 temperature and relative humidity were monitored. Three PM_{2.5} pollution episodes were analysed. In
24 episode 1 (October 27th to November 1st), regional transport accompanied with the accumulation of
25 pollutants under unfavourable meteorological conditions led to the pollution. In episode 2 (November
26 2nd to 5th), pollutants left from episode 1 were retained in the boundary layer for 2 days in the region
27 and then settled down to the surface, leading to an explosive increase of PM_{2.5}. The regional transport
28 of aged aerosols played a crucial role in the heavy PM_{2.5} pollution. In episode 3 (November 6th to 11th),
29 emission from large point sources had been controlled for several days while primary emissions from
30 diesel vehicle might lead to the pollution. It is found that ground-level observation of meteorology
31 condition and air quality could not fully explain the pollution process while vertical parameters



- 1 (aerosol optical profile, wind profile, relatively humidity profile and temperature profile) improved
- 2 the understanding of regional transport influence on heavy pollution process. Further vertical
- 3 observations are needed to investigate the pollutants transport especially during the explosive increase
- 4 pollution episode.



1 1. Introduction

2 With a rapid economic development and increases in energy consumption, large quantity of emissions
3 has caused serious air pollution in China. Monitoring data show that Beijing-Tianjin-Hebei (BTH)
4 region is one of the most polluted region in China (Zhao et al., 2013; Wang et al., 2014). The region
5 was home to eight out of the top 10 most polluted Chinese cities in 2014 (MEP-Ministry of
6 Environment Protection, 2015). In 2014, the annual average PM_{2.5} (particulate matter with
7 aerodynamic diameter less than 2.5 μm) concentration reached 95 μg/m³ in the BTH region. With
8 21.5 million residents and 5.3 million vehicles, Beijing has been burdened with severe pollution
9 episodes frequently in recent years (Beijing Municipal Bureau of Statistics, 2014). The capital is
10 surrounded by mountains in three directions (north, west and east). The top three most polluted cities
11 in China (Baoding, Xingtai and Shijiazhuang) are located in the south to Beijing. Polluted air mass
12 from the south contributes to PM_{2.5} pollution in Beijing (Wang et al., 2015). Source apportionment by
13 Beijing Environmental Protection Bureau indicates regional transport contributed 28%-36% to PM_{2.5}
14 in Beijing in 2012-2013. During some severe pollution periods, regional contribution was more than
15 50% (<http://www.bjepb.gov.cn/bjepb/413526/331443/331937/333896/396191/index.html>). Quite a
16 few researches have studied the causes of heavy polluted episodes in BTH region and show regional
17 transport plays an important role in pollution formation. The sharp PM_{2.5} build-up events in Beijing
18 were unique while accumulation pollution process occurred at other cities in the region. This
19 indicated that PM_{2.5} was probably transported to Beijing from other cities (Zheng et al., 2015; Ji et al.,
20 2014; Tao et al, 2014; Zhao et al., 2013). In the meanwhile, most severe pollutions are under stable
21 synoptic meteorological conditions in Beijing (Sun et al., 2015; Zheng et al., 2015; Zhao et al., 2013).
22 The low wind speed and stable synoptic meteorological condition at ground level cannot explain the
23 reason that regional transport makes significant contribution to severe pollution. A previous study has
24 shown the secondary aerosol in Beijing probably mainly formed over regional transport according to a
25 vertical observation from the ground to 260m height. (Sun et al., 2015). Therefore, vertical profiles of
26 meteorology and air quality might help us to understand the impacts of regional transport to heavy
27 pollution during stagnant conditions.

28 As in other megacities with local sources and regional transport, air quality in Beijing are affected by
29 many factors, including emissions inside the city, formation of secondary pollutants, atmospheric
30 mixing, and regional transport. It has been well known that the strength of each factor varies
31 according to emissions and/or weather conditions. Therefore, it is challenging to pin point the major
32 contributors in any given time periods, either clean or polluted episodes. This is especially difficult in
33 BTH region considering the complicated emission sources and transport processes.



1 Emission control measures implemented during some events provide a unique opportunity to
2 investigate the impact of various factors influencing air quality. One of them was APEC (Asia-Pacific
3 Economic Cooperation) Economic Leaders' 2014 Summit held in Beijing from November 5th to 11th,
4 2014. A strict air pollution control plan was carried out in the BTH Region to improve air quality in
5 Beijing from November 2nd to 11th for APEC. According to a conservative estimate by MEP,
6 production of 9,289 plants were paused and 3900 plants were running at reduced capacity in six
7 provinces (Beijing, Tianjin, Hebei, Shanxi, Shandong and Inner Mongolia); and more than 40
8 thousand construction sites were shut down temporarily
9 (http://www.zhb.gov.cn/gkml/hbb/qt/201411/t20141115_291482.htm). Other measures include traffic
10 control (50% of private passenger vehicles and 70% of buses were off-road) and frequent road
11 sweeping and cleaning in Beijing. More detail emission control measures are supplied in the
12 supporting information. Studies have found that regional emission control effectively reduced air
13 pollutant concentrations during the Summit (Wen et al., 2015; Tang et al., 2015; Han et al., 2015;
14 Chen et al., 2015; Sun et al., 2016a). The significantly reduced local emissions led to reduced
15 complexity of pollution process, thus providing a unique opportunity to investigate the influence of
16 transport events on PM_{2.5} levels in Beijing.

17 The objective of the study is to investigate the impact of regional transport on PM_{2.5} in Beijing using
18 both ground-level and vertical observations. Field observation was conducted at a rural site (Liulihe)
19 in southwest Beijing before and during the control period of the APEC 2014 Summit. Vertical profiles
20 of temperature, RH (relative humidity), wind speed and direction, and extinction coefficient were
21 observed as well as pollutants concentration and meteorological parameters on the ground. The
22 characteristics of three PM_{2.5} pollution episodes were analysed. Findings of this study will help
23 explore vertical observation methods for in-depth analysis of the meteorological and transport
24 influence. Furthermore, it can aid the development of future air quality management strategies in BTH
25 and other regions around the globe, including emission control and air surveillance.

26 **2. Field observation and analysis methods**

27 **2.1 Field observation site and sampling methods**

28 Beijing is surrounded by mountains in the west, north and east directions, which blocks the pollutants
29 from spreading. The open air corridor in the south exposes the capital to air mass passing Hebei
30 Province (Fig. S1) a heavily polluted area in China. To investigate the impact of regional transport on
31 Beijing, a rural site (Liulihe site, 116°2'E, 39°36'N) was chosen in the southwest of Beijing. It was
32 located on the border of Beijing and Hebei Province (Fig. S1).



1 The field campaign was conducted from October 27th to November 12th, 2014, including both ground-
2 level and vertical observations. Detailed information of instruments at Liulihe site is provided in
3 Table S1. Ground-level observations included meteorological parameters, mass concentration of
4 PM_{2.5}/PM₁₀, SO₂, NO_x and O₃ as well as physical and chemistry properties of PM. PM_{2.5}/PM₁₀ mass
5 concentration was determined by the TEOM method. Particle size distribution from 3nm to 10µm
6 were measured by a spectrometer assembled in-house including one Nano scanning mobility particle
7 sizers (NSMPS), one scanning mobility particle sizers (SMPS), and one aerodynamic particle sizer
8 (APS) (Liu et al., 2014).

9 ACSM (Aerosol Chemical Speciation Monitor), a low-maintenance aerosol mass spectrometer, was
10 used to measure non-refractory (NR) particulate matter with aerodynamic diameters smaller than 1µm
11 (PM_i) (Ng et al., 2011). The ACSM data was calibrated with a collection efficiency (CE) value to
12 compensate for the particle loss. The CE value of 0.45 recommended by Middlebrook et al. (2012)
13 based on the monitoring site condition (see supporting information) was used in this study. The NR-
14 PM₁ concentration measured by ACSM tracks well with PM_{2.5} measured by the TEOM (R²=0.91) and
15 the regression slope is 0.43 (Fig. S2). Positive matrix factorization (PMF) with the PMF2.exe
16 algorithm was used to distinguish different components of OA measured by ACSM (Paatero and
17 Tapper, 1994). The PMF was performed and evaluated following the PMF analysis guide
18 (http://cires1.colorado.edu/jimenez-group/wiki/index.php/PMF-AMS_Analysis_Guide). Three factors
19 were distinguished (Fig. S3), i.e., HOA (hydrocarbon-like organic aerosol), SVOOA (semi volatility
20 oxygenated organic aerosol) and LVOOA (low volatility oxygenated organic aerosol).

21 Beyond ground-level concentrations of routinely monitored air pollutants and meteorological
22 parameters, the assessment was aided by vertical observations including vertical extinction coefficient
23 profile, as well as vertical wind, RH and temperature profiles. The vertical extinction coefficient
24 profiles depict the distribution of PM, which could be used to infer mixing process of particles
25 transported in from high elevations and those near the ground. Vertical wind profile can help figure
26 out the transport direction. Vertical RH profile can provide the RH information at transport layers,
27 thus helping investigate heterogeneous reaction at the layers. Vertical temperature profiles provide
28 information on the stability of and mixing in the boundary layer. Lidar was used to observe the
29 vertical optical properties of atmospheric aerosols at Liulihe site. The lidar consists of three parts,
30 including emitting system, receiving system and signal analogue system (Chen et al., 2015). The laser
31 source emitted pulse at 355/532nm. The pulse energy is 30MJ at 355nm and 20MJ at 532nm. The
32 pulse repetition is 20Hz. The telescope for receiving system is based on a Cassegrain design.
33 Diameter of the telescope is 200mm with a vertical resolution of 7.5m. The particle backscatter



1 coefficient and extinction coefficient was retrieved by Fernald method (Fernald et al., 1984). CFL-03
2 phased array wind profile radar was used to monitor the vertical wind speed and direction with
3 resolutions of 50 m (0-1 km) and 100 m (1-5.5 km). Parameters of these instruments can be found in
4 another paper (Wang et al., 2013). Vertical profiles of atmospheric temperature and humidity were
5 derived by profiling radiometers. The channel centre frequencies were 22-32 GHz (K-Band) and 51-
6 59 GHz (V-Band). The vertical resolutions were 60 m (0-4 km) and 120 m (4-10 km).

7 2.2 Back trajectory analysis

8 Trajstat, a GIS-based software into which the HYSPLIT (Hybrid Single Particle Lagrangian
9 Integrated Trajectory) model was loaded (Wang et al., 2009), was used to calculate the back trajectory.
10 The model was run every 6 hours in a 24-hour mode back-trajectory mode at 1000 m above sea level
11 from Liulihe site to identify the origins and path way of air mass. The meteorology data used in the
12 mode was obtained from the Global Data Assimilation System (GDAS) model
13 (<http://www.ready.noaa.gov/READYamet.php>).

14 2.3 Quantification of regional transport contribution

15 A novel technique was used to quantify the contribution of regional transport. The diurnal trend of
16 PM_{2.5} in Beijing often exhibit “Saw-tooth cycles” with a smoothly increasing or decreasing baseline
17 upon which daily cycles are superimposed. Ancillary measurements around Beijing show that the
18 baselines represent regional aerosols, while the daily cycles represent local aerosols. Following Jia et
19 al. (2008), the total contribution is defined as the area under the concentration line (A_t), while its
20 regional component is defined as the area under the baseline curve (A_r). Both areas are approximated
21 using trapezoid numerical integration as Eq. (1):

$$22 \quad A_N = \sum_{n=1}^{N-1} A_i = \sum_{n=1}^{N-1} \frac{(C_i + C_{i+1})}{2} \times (t_{i+1} - t_i) \quad (1)$$

23 Where N is the total number of hourly PM_{2.5} concentrations in a specific time period, C_i is total
24 concentration (for A_t) or baseline concentration (for A_r) value at time t_i ($i=1, N-1$). The baseline
25 concentration curve is the line connecting daily afternoon minimal values. The percentage regional
26 contribution (R) is expressed as following Eq. (2):

$$27 \quad R = \frac{A_r}{A_t} \times 100\% \quad (2)$$



1 3. Results and discussion

2 3.1 General characteristics of atmospheric pollution before and during APEC summit

3 To investigate the changes in air quality during APEC summit, average pollutant concentrations and
4 the rates of changes were calculated. Period 1 (October 27th to November 2nd) and period 2
5 (November 3rd to November 12th) were defined to represent the periods before and during the APEC
6 summit. Concentrations of PM_{2.5}, SO₂ and NO₂ decreased significantly during the emission control
7 (Period 2) compared to before control (Period 1) as shown in Fig. S4 (a). The large rates of reduction
8 were observed for NO₂ (37%) and SO₂ (36%), while the reduction in PM_{2.5} was smaller (21%) but still
9 significant (Fig. S4 (b)).

10 Three pollution episodes were selected to discuss the pollution characteristics during the observation
11 (Fig. S5). PM_{2.5} concentration at Miyun site (locate in northern Beijing, shown in Fig. S1, data source:
12 Beijing EPB) is shown in Fig. S5 alongside Luilihe to demonstrate the synchronism of PM_{2.5} levels at
13 different sides in Beijing. Episode 1 (October 27th to November 1st) represents the period before the
14 emission control. Episode 2 (November 2nd to 5th) was the first pollution episode during the emission
15 control plan. Episode 3 (November 6th to 11th) was the second pollution episode during the emission
16 control plan. At Luilihe, PM_{2.5} concentration was the highest in episode 1 (140±70µg/m³) before
17 implementation of emission control, whereas the mean values were close during the last two episodes
18 (91±75µg/m³ and 89±61µg/m³).

19 The average concentration of online PM₁ chemical components was shown in Fig. 1. Average
20 concentrations of OM (organic matter), NH₄⁺, SO₄²⁻ and NO₃⁻ were the highest in episode 1 before
21 emission control. During episode 2, those compounds decreased by 32-60%. In episode 3, the average
22 concentrations remained similar except NH₄⁺ which decreased by 12%. HOA (related to primary
23 emission), LVOOA and SVOOA were distinguished. Compared with episode1, the HOA, LVOOA
24 and SVOOA decreased by 22%, 58% and 28% in episode 2. After that, LVOOA kept decreasing by
25 10% in episode 3 while HOA and SVOOA increased by 39% and 5%.

26 Overall, most meteorological parameters changed little during the three episodes except RH (Fig. S6)).
27 The average ground-level RH (69%) in episode 1 was higher compared with those in episode 2 (50%)
28 and in episode 3 (58%). Wind speed remained low during the entire observation. The average wind
29 speed was 0.5m/s, 0.8m/s and 0.7m/s in episode 1, episode 2 and episode 3, respectively. The
30 dominant wind direction was southwest during the 10-day observation. The frequency of southwest



1 wind was above 60% during each of the three episodes, with the highest occurrence of 81% observed
2 during episode 2.

3 The significant reduction in pollutant concentrations during APEC shown above implied that the
4 emission control was effective. However, the general characteristics derived from ground-level
5 observation are insufficient to identify the leading cause of air pollution, local emissions, regional
6 transport, or both. Furthermore, the significant differences of particle chemical components changes
7 from episode 2 to episode 3 under similar ground-level meteorological conditions and local emission
8 intensity suggest different transport or formation mechanisms during those two episodes. Therefore,
9 vertical observations will be used to aid further investigation in each of the three episodes in the
10 following section.

11 **3.2 Characteristics of heavy PM_{2.5} pollution episodes and contribution of regional transport**

12 **3.2.1 Pollution process in episode 1**

13 Episode 1 (October 27th to November 1st) was before emission control. The high level of PM_{2.5} is
14 typical in Beijing during the autumn. There were two unique features in this episode. One is the
15 continued increases of PM_{2.5} mass and PM₁ component concentrations during the first four days, with
16 OM showing a more distinct diurnal cycle (Fig. 2, Fig. 3 and Fig. S5). Another is the rapid increase of
17 OM on Oct 29th (Fig. 3). Both suggest except secondary formation, other mechanisms might impact
18 the OM growth and needs further investigation.

19 Various parameters collected during episode 1 are shown in Fig. 4. Combining the ground-level
20 observation and vertical observation, it is evidenced that the pollution was caused by the regional
21 transport and pollutants accumulation later. Vertical extinction coefficient data observed at
22 Yongledian site (116°47'E, 39°43'N) near Liulihe site were used (Fig. 4(a)), because the optical lidar
23 at Liulihe didn't work in October. High level of PM appeared at approximately 2 km above ground
24 (Fig. 4 (a)) and retained there for 1 day. The air mass came from the southwest where emissions were
25 high (see horizontal wind direction profile, Fig. 4 (c)). Back trajectories also show air mass from
26 southwest arrived in Liulihe, as well as Yongledian (Fig. S7). Then pollutants settled down (see
27 downward vertical wind direction in Fig. 4 (b)) and mixed with aerosols on the ground (Fig. 4 (a)).
28 The online particle size distribution also implied the transport process. During the same period (from
29 13:00 to 20:00 on October 28th), a new group of particles appeared and mixed with existing particles,
30 indicating the arrival of aged aerosols (Fig. 4 (e)). As mentioned above, except secondary formation,
31 other mechanisms might impact OM increase. The increase of OM might come from freshly-emitted



1 organic particles and transported to the site instead of aged particles. One evidence is that both HOA
2 and OOA increased significantly. Another is that the OM peak appeared after the transport occurrence,
3 much earlier than SNA. It is noticed, even wind direction on the ground changed to north in the early
4 morning on October 29th, it still kept in the southwest above 500m, indicating significant influence of
5 regional transport.

6 In the next two days (October 30th to 31st), vertical wind direction was downward and pollutants were
7 easily accumulated in the boundary layer (Fig. 5). Meanwhile, high RH on the surface (Fig. S6)
8 enhanced the formation of SA (secondary aerosol) as pointed out by Pathak et al. (2009). Under this
9 condition, NH_4^+ , SO_4^{2-} and NO_3^- concentrations increased at rates of $0.26\mu\text{g}/\text{m}^3/\text{h}$, $0.21\mu\text{g}/\text{m}^3/\text{h}$, and
10 $0.58\mu\text{g}/\text{m}^3/\text{h}$, respectively. The peak of NH_4^+ , SO_4^{2-} and NO_3^- concentrations was two days later than
11 OM. This also proved the organic particles were transported to Beijing and reached to the peak on
12 October 29th and secondary formation became severe later, both of which promoted the pollution
13 occurrence.

14 To quantify the impacts of regional transport, the transport component is calculated with the method
15 introduced in section 2.2. The baseline needs to be defined first especially for pollution end timing.
16 Here the vertical observation and ground observation were combined to discuss when the pollution
17 ended. In the morning on 1st November, air mass from the north above 1000 m arrived Beijing. The
18 vertical temperature gradient decreased and vertical mixing became weak (wind vertical speed was
19 very low). Consequently, $\text{PM}_{2.5}$ accumulated and had a sharp increase. Then clean and cold wind from
20 north caused sharp increase of wind speed and decrease of atmosphere pressure. Based on the analysis
21 above, pollution ended up at 18:00 when the weak temperature ended and $\text{PM}_{2.5}$ decreased sharply
22 (Fig. 6). The regional component is calculated based on the determination of baseline.

23 For episode 1, the regional component accounted for 75%, indicating the important influence of
24 regional transport on the pollution. It can be seen that episode 1 was a pollution episode influenced by
25 transport process in Beijing. RH was high, wind speed kept low and wind direction was dominated by
26 southwest in the surface. Vertical observation showed pollutants transported from southwest settled
27 down. OM concentration increased significantly when the transport PM was observed. After that
28 vertical wind direction kept downward and promoted the pollutants accumulation, especially SNA.

29 3.2.2 Pollution process in episode 2

30 Episode 2 (November 2nd to 5th) saw a lower mean $\text{PM}_{2.5}$ concentration ($91\pm 75\mu\text{g}/\text{m}^3$) due to the
31 implementation of emission control since November 2nd. Unlike the gradual accumulation of PM



1 observed in episode 1, $PM_{2.5}$, OM and SNA had a sharp increase from November 4th to 5th. The
2 concentrations of NH_4^+ , SO_4^{2-} and NO_3^- increased at rates from the lowest to the highest of
3 $0.88\mu g/m^3/h$, $0.43\mu g/m^3/h$, and $1.64\mu g/m^3/h$, respectively, much faster than that in episode 1. OOA
4 also increased much more significantly during this episode. The explosively increases of PM
5 components mainly SA in such a short period of time is contrary to lower RH values in this episode
6 leading to less heterogeneous reaction. Thus, such rapid increases in PM levels could be transport of
7 aged aerosol from other regions, as hypothesized by previous studies where the transport process
8 wasn't observed directly (Yue, et al., 2009; Massling., et al, 2009; Sun et al., 2014; Sun et al., 2016b).

9 With the aid of vertical observation, an in-depth investigation revealed atmospheric processes leading
10 to the peak concentrations during November 4th to 5th. Firstly, after the end of episode 1 at November
11 1st, relatively high PM levels still resided at 1000m (from November 2nd to 3rd) as shown in the
12 vertical extinction coefficient (Fig. 7). Furthermore, a band of high PM centered around 750 m were
13 observed ((Fig. S8) on November 3rd at another site (Baoding site, 115°31'E, 38°52'N, shown in Fig.
14 S1) in the BTH region, suggesting a wide-spread PM aloft in the region. During the next two days, the
15 pollutants were transported in the region and the slow winds (average speed of 4.8m/s at 1000 m)
16 allowed aerosols ample time to age in their journey. Back trajectories showed transport of air mass
17 from the southwest at the night of November 3rd (Fig. S9), consistent with the vertical wind profile
18 observed at Liulihe (Fig. 8 and Fig.9). On November 4th, the downward motion of air mass around
19 1000 m above ground intensified, bringing the aged aerosols down and mixing them with the aerosols
20 on the ground. The well mixed boundary layer with regard to aerosol is evidence in Fig. 9 with a
21 fairly uniform distribution from the ground to 900 m. Consequently, secondary chemical component
22 concentrations of PM_1 (Fig. 2 and Fig. 3) started ascending with remarkably fast rates.

23 Dry and clean wind from north direction arrived in the early morning on November 5th. RH started to
24 increase significantly at 10:00 and wind speed became higher from 12:00. At the same time, $PM_{2.5}$
25 concentration started to decrease. Based on the analysis, the pollution ended up at 12:00. The
26 calculation shows regional transport contributed 62%, relatively lower than that during episode 1 (Fig.
27 6).

28 Rather than chemical reaction, aged aerosols settled down and had important contribution to the
29 pollution in episode 2. Vertical observations found that the aged aerosol settled down and caused the
30 explosive increase of SNA in such a short time, which can't be explained by the ground-level
31 observations. It was also noticed that the pollution occurred when the emission control plan just
32 started, which means this episode was partly caused by regional transport before control. Even when



1 local emission control was conducted effectively, the uncontrolled regional emission still led to severe
2 pollution in Beijing.

3 **3.2.3 Pollution process in episode 3**

4 During episode 3 (November 6th to 11th), Lulihe site recorded a relatively high average PM_{2.5}
5 concentration of 89±61 μg/m³. Furthermore, this episode is characterized by much more and faster
6 increases in OM concentrations than SNA (Fig. 2 and Fig. 3). Specifically, concentrations of aerosol
7 related with fuel combustion (HOA) increased significantly. While SNA increased slowly (NH₄⁺ and
8 NO₃⁻) or changed little (SO₄²⁻). All of these indicate primary emission rather than the formation of SA
9 was the dominant cause.

10 Vertical extinction coefficient shows pollutants appeared at 2000-2500m on November 7th. The air
11 mass came from the northwest and the vertical convection bringing them down on November 7th and
12 8th (Fig. 7, Fig. 8 and Fig. 10). Air mass trajectories at 1000 m also show air mass arrived in Beijing
13 from the south on November 7th but changing to the northwest on November 8th (Fig. S10). Because
14 the northwest was less polluted and the effective emission control in BJH region during the APEC,
15 the regional transport of PM was weakened. This is supported by an estimated regional contribution
16 of 53% to PM_{2.5} in Beijing, much lower than in episode 1 (75%) and episode 2 (63%).

17 Figure 11 depicts black carbon (BC) concentrations measured by Aethalometer and OM
18 concentrations measured by ACSM. They tracked each other well during this episode. Concentrations
19 of BC, a marker of vehicular emission in urban settings, had two peaks every day. One was in the
20 early morning and another was in the morning rush hour of 9:00am. The first peak might result from
21 diesel vehicle emissions (Westerdahl, et al., 2009). This is because transportation of goods to Beijing
22 via heavy-duty diesel vehicles has been permitted at night only, and the number of trucks was large.
23 When the regional emission control was conducted effectively and air mass was from relatively clean
24 areas, traffic emissions in and around the city became the dominant source.

25 **4. Conclusion**

26 This study indicates that the meteorology condition on the ground sometime couldn't explain the
27 pollution process, especially the pollutions impacted by transport significantly. Vertical observation
28 can provide the vertical meteorological and optical profile, which can help identify the regional
29 transport episodes. Combining the ground-level observation with information from radars, we can
30 determine the regional transport influence on air quality.



1 Three episodes of different types under similar ground meteorological condition were discussed in
2 this study. In episode 1, particle concentration accumulated under the unfavorable meteorological
3 condition after transport occurred. The transport pollutants brought organic aerosol and SNA
4 increased under high RH later. In episode 2, pollutants left from episode 1 kept in the boundary layer
5 in the region. When vertical wind direction changed to downward, the pollutants were settled down.
6 As a result, OM and SNA increased much explosively. In episode 3, when control plan had been
7 conducted for several days, SNA and OA concentration increased much less while HOA and
8 increased significantly. The pollution might be caused by the primary emission from diesel vehicles.

9 Our research suggests regional transport of air pollutants has significant contribution (up to 70%) to
10 severe secondary particle pollution, even when local emission was controlled effectively (53%, such
11 as in APEC summit). Although lots of efforts were paid to air quality management in Beijing, the
12 equal efforts need to be paid to regional emission to ensure the clean air. What's more, diesel vehicle
13 emission at night in Beijing might be an important pollution source and needs further investigation.

14 **5. Acknowledgements**

15 This work was supported by the MEP's Special Funds for Research on Public Welfare (201409002),
16 Strategic Priority Research Program of the Chinese Academy of Sciences (XDB05020300), and
17 National Natural Science Foundation of China (21521064). The authors also appreciate the support
18 from Collaborative Innovation Center for Regional Environmental Quality.

19



1 **References**

- 2 Ng, N.L., Herndon, S.C., Trimborn, A., Canagaratna, M.R., Croteau, P.L., Onasch, T.B., Sueper, D.,
3 Worsnop, D.R., Zhang, Q., Sun, Y.L. and Jayne, J.T. (2011) An Aerosol Chemical Speciation
4 Monitor (ACSM) for Routine Monitoring of the Composition and Mass Concentrations of
5 Ambient Aerosol. *Aerosol Science and Technology* 45(7), 780-794.
- 6 Beijing Municipal Bureau of Statistics, The national statistical yearbook of China in 2014, 2015.
- 7 Chen, C., Sun, Y., Xu, W., Du, W., Zhou, L., Han, T., Wang, Q., Fu, P., Wang, Z. and Gao, Z. (2015)
8 Characteristics and sources of submicron aerosols above the urban canopy (260 m) in Beijing,
9 China, during the 2014 APEC summit. *Atmos. Chem. Phys* 15(22), 12,879-812,895..
- 10 Chen, Z., Zhang, J., Zhang, T., Liu, W. and Liu, J. (2015) Haze observations by simultaneous lidar
11 and WPS in Beijing before and during APEC, 2014. *Science China Chemistry* 58(9), 1385-1392.
- 12 Frederick G. Fernald. (1984) Analysis of atmospheric lidar observation: some comments. *Applied*
13 *Optics* 84(23), 652-653.
- 14 Han, T., Xu, W., Chen, C., Liu, X., Wang, Q., Li, J., Zhao, X., Du, W., Wang, Z. and Sun, Y. (2015)
15 Chemical apportionment of aerosol optical properties during the Asia - Pacific Economic
16 Cooperation (APEC) summit in Beijing, China. *Journal of Geophysical Research: Atmospheres*
17 120(23), 12281-12295.
- 18 Ji, D., Li, L., Wang, Y., Zhang, J., Cheng, M., Sun, Y., Liu, Z., Wang, L., Tang, G., Hu, B., Chao, N.,
19 Wen, T. and Miao, H. (2014) The heaviest particulate air-pollution episodes occurred in northern
20 China in January, 2013: Insights gained from observation. *Atmospheric Environment* 14(92),
21 546-556.
- 22 Jia, Y., Rahn, K.A., He, K., Wen, T. and Wang, Y. (2008) A novel technique for quantifying the
23 regional component of urban aerosol solely from its sawtooth cycles. *Journal of Geophysical*
24 *Research: Atmospheres* 113(D21).
- 25 Liu, J., Jiang, J., Zhang, Q., Deng, J. and Hao, J. (2014) A spectrometer for measuring particle size
26 distributions in the range of 3 nm to 10 μm. *Frontiers of Environmental Science & Engineering*
27 16(10), 63-72.



- 1 Massling, A., Stock, M., Wehner, B., Wu, Z., Hu, M., Brüggemann, E., Gnauk, T., Herrmann, H. and
2 Wiedensohler, A. (2009) Size segregated water uptake of the urban submicrometer aerosol in
3 Beijing. *Atmospheric Environment* 43(8), 1578-1589.
- 4 Middlebrook, A.M., Bahreini, R., Jimenez, J.L. and Canagaratna, M.R. (2012) Evaluation of
5 composition-dependent collection efficiencies for the aerodyne aerosol mass spectrometer using
6 field data. *Aerosol Science and Technology* 46(3), 258-271.
- 7 Paatero, P. and Tapper, U. (1994) Positive matrix factorization: A non - negative factor model with
8 optimal utilization of error estimates of data values. *Environmetrics* 5(2), 111-126.
- 9 Pathak, R.K., Wu, W.S. and Wang, T. (2009) Summertime PM_{2.5} ionic species in four major cities of
10 China: nitrate formation in an ammonia-deficient atmosphere. *Atmospheric Chemistry and
11 Physics*, 9(5), 1711-1722.
- 12 Tang, G., Zhu, X., Hu, B., Xin, J., Wang, L., Münkel, C., Mao, G. and Wang, Y. (2015) Impact of
13 emission controls on air quality in Beijing during APEC 2014: lidar ceilometer observations.
14 *Atmospheric Chemistry and Physics* 15(21), 12667-12680.
- 15 Sun, Y., Jiang, Q., Wang, Z., Fu, P., Li, J., Yang, T. and Yin, Y. (2014) Investigation of the sources
16 and evolution processes of severe haze pollution in Beijing in January 2013. *Journal of
17 Geophysical Research: Atmospheres* 119(7), 4380-4398.
- 18 Sun, Y., Du, W., Wang, Q., Zhang, Q., Chen, C., Chen, Y., Chen, Z., Fu, P., Wang, Z. and Gao, Z.
19 (2015) Real-Time Characterization of Aerosol Particle Composition above the Urban Canopy in
20 Beijing: Insights into the Interactions between the Atmospheric Boundary Layer and Aerosol
21 Chemistry. *Environmental Science & Technology* 49(19), 11340-11347.
- 22 Sun, Y., Wang, Z., Wild, O., Xu, W., Chen, C., Fu, P., Du, W., Zhou, L., Zhang, Q. and Han, T.
23 (2016a) "APEC Blue": Secondary Aerosol Reductions from Emission Controls in Beijing.
24 *Scientific reports* 6, 20668.
- 25 Sun, Y., Chen, C., Zhang, Y., Xu, W., Zhou, L., Cheng, X., Zheng, H., Ji, D., Li, J. and Tang, X.
26 (2016b) Rapid formation and evolution of an extreme haze episode in Northern China during
27 winter 2015. *Scientific reports* 6, 27151.
- 28 Tao, M., Chen, L., Xiong, X., Zhang, M., Ma, P., Tao, J. and Wang, Z. (2014) Formation process of
29 the widespread extreme haze pollution over northern China in January 2013: Implications for
30 regional air quality and climate. *Atmospheric Environment* 98, 417-425.



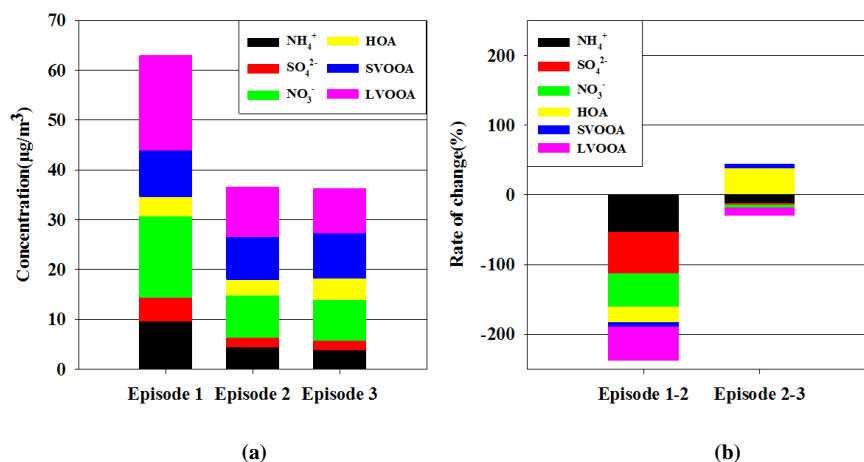
- 1 Wang, J., Wang, S., Jiang, J., Ding, A., Zheng, M., Zhao, B., Wong, D.C., Zhou, W., Zheng, G. and
2 Wang, L. (2014) Impact of aerosol–meteorology interactions on fine particle pollution during
3 China’s severe haze episode in January 2013. *Environmental Research Letters* 9(9), 094002.
- 4 Wang, L., Liu, Z., Sun, Y., Ji, D. and Wang, Y. (2015) Long-range transport and regional sources of
5 PM_{2.5} in Beijing based on long-term observations from 2005 to 2010. *Atmospheric Research* 157,
6 37-48.
- 7 Wang, M., Wei, W., Ruan, Z., He, Q. and Ge, R. (2013) Application of wind-profiling radar data to
8 the analysis of dust weather in the Taklimakan Desert. *Environmental monitoring and
9 assessment* 185(6), 4819-4834.
- 10 Wang, Y., Zhang, X. and Draxler, R.R. (2009) TrajStat: GIS-based software that uses various
11 trajectory statistical analysis methods to identify potential sources from long-term air pollution
12 measurement data. *Environmental Modelling & Software* 24(8), 938-939.
- 13 Wen, W., Cheng, S., Chen, X., Wang, G., Li, S., Wang, X. and Liu, X. (2015) Impact of emission
14 control on PM_{2.5} and the chemical composition change in Beijing-Tianjin-Hebei during the
15 APEC summit 2014. *Environmental science and pollution research* 23(5) 4509-4521.
- 16 Westerdahl, D., Wang, X., Pan, X. and Zhang, K.M. (2009) Characterization of on-road vehicle
17 emission factors and microenvironmental air quality in Beijing, China. *Atmospheric
18 Environment* 43(3), 697-705.
- 19 Yue, D., Hu, M., Wu, Z., Wang, Z., Guo, S., Wehner, B., Nowak, A., Achtert, P., Wiedensohler, A.
20 and Jung, J. (2009) Characteristics of aerosol size distributions and new particle formation in the
21 summer in Beijing. *Journal of Geophysical Research: Atmospheres* 114(D2).
- 22 Zhang, Z.Y., Wong, M.S. and Lee, K.H. (2015) Estimation of potential source regions of PM_{2.5} in
23 Beijing using backward trajectories. *Atmospheric Pollution Research* 6(1), 173-177.
- 24 Zhao, B., Wang, S., Dong, X., Wang, J., Duan, L., Fu, X., Hao, J. and Fu, J. (2013) Environmental
25 effects of the recent emission changes in China: implications for particulate matter pollution and
26 soil acidification. *Environmental Research Letters* 8(2), 024031.
- 27 Zhao, X., Zhao, P., Xu, J., Meng, W., Pu, W., Dong, F., He, D. and Shi, Q. (2013) Analysis of a
28 winter regional haze event and its formation mechanism in the North China Plain. *Atmospheric
29 Chemistry and Physics* 13(11), 5685-5696.



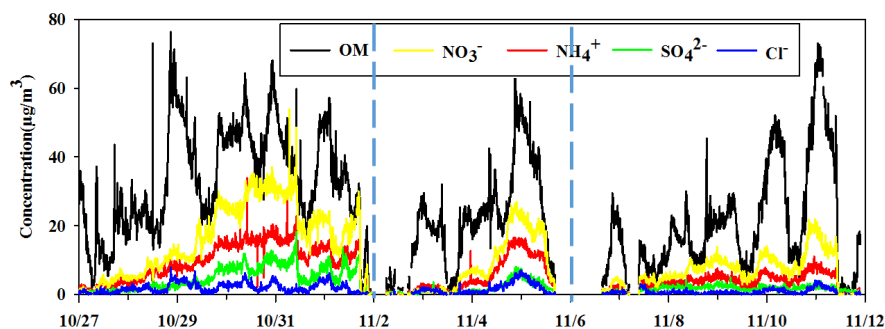
- 1 Zheng, G.J., Duan, F.K., Su, H., Ma, Y.L., Cheng, Y., Zheng, B., Zhang, Q., Huang, T., Kimoto, T.,
- 2 Chang, D., Poeschl, U., Cheng, Y.F. and He, K.B. (2015) Exploring the severe winter haze in
- 3 Beijing: the impact of synoptic weather, regional transport and heterogeneous reactions.
- 4 Atmospheric Chemistry and Physics 15(6), 2969-2983.



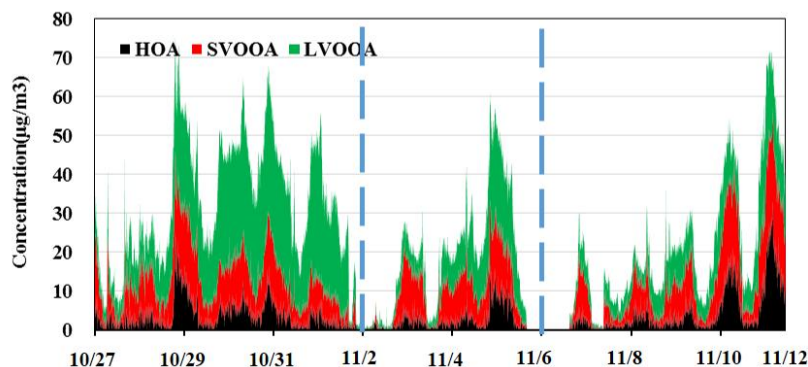
1 **Figures**



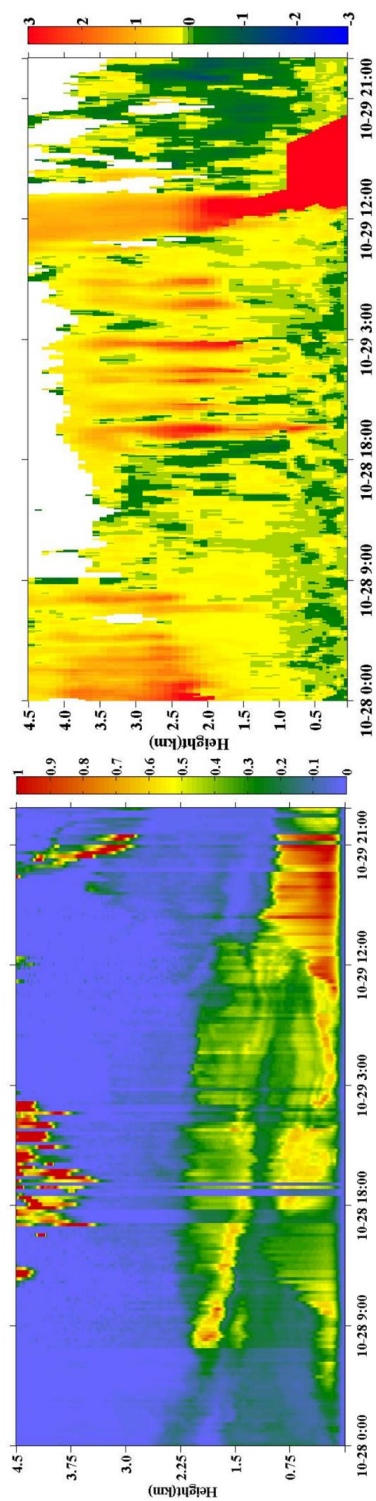
2
 3
 4 **Figure 1. Average PM₁ chemical components and the change rates during different episodes (a)**
 5 **average PM₁ chemical components; (b) change rates in chemical components**



6
 7 **Figure 2. PM₁ chemical components during the observation at Liulihe site**

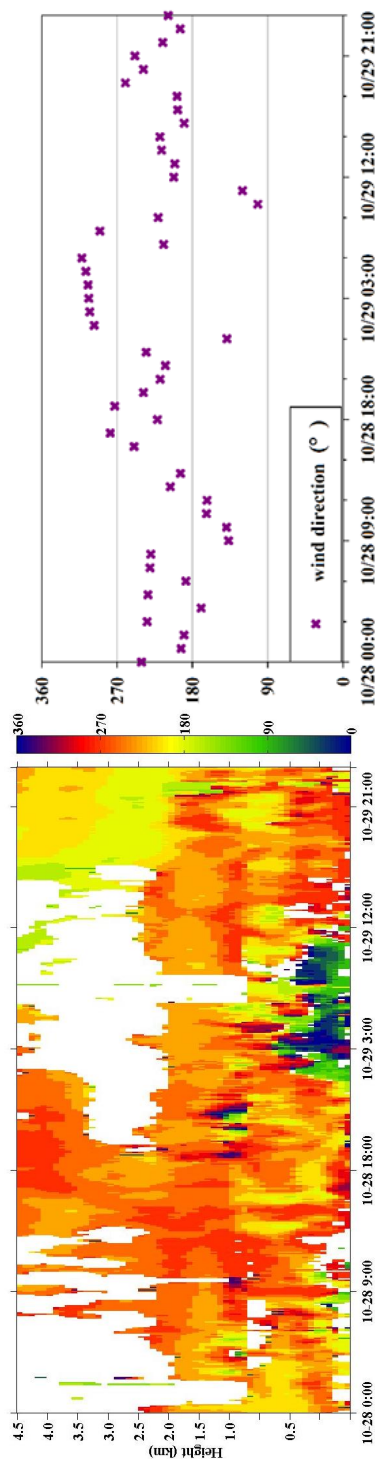


8
 9 **Figure 3. PM₁ organic components during the observation at Liulihe site**



(b)

(a)



(d)

(c)

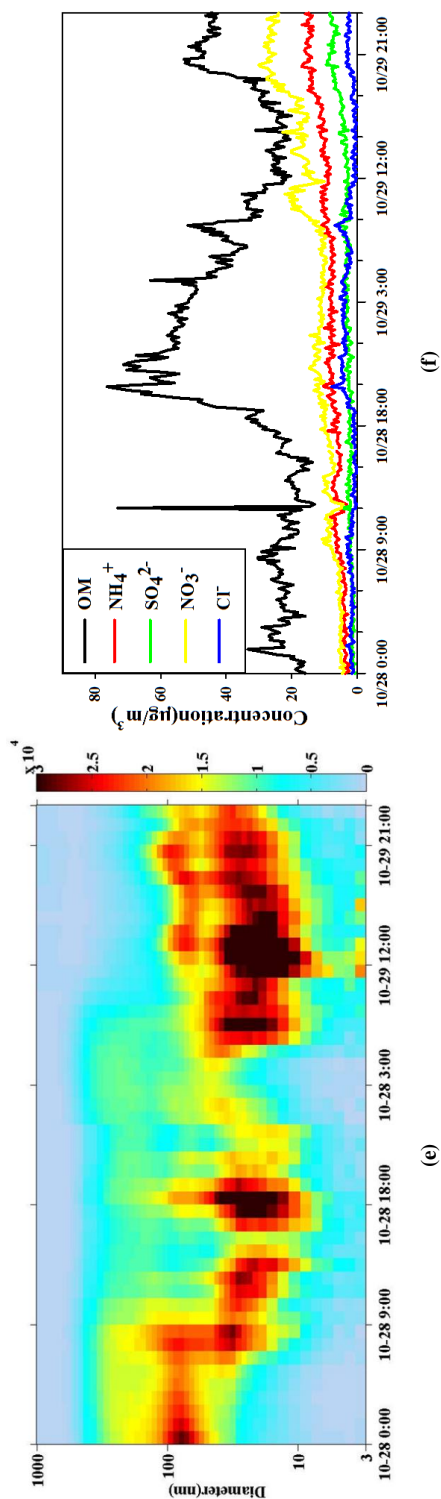


Figure 4. Parameters of particles and meteorology during episode 1

(a) Vertical profile of extinction coefficient (km⁻¹) (Yongliedan site); (b) Vertical profile of wind vertical direction and speed (m/s, positive stands for up, negative stands for down); (c) Horizontal wind direction profile (°; 0° stands for north); (d) wind direction on the ground; (e) Particle size distribution (dN/dlogDp, N: number concentration (cm⁻³); Dp: particle diameter (nm)); (f) PM₁ chemical components.

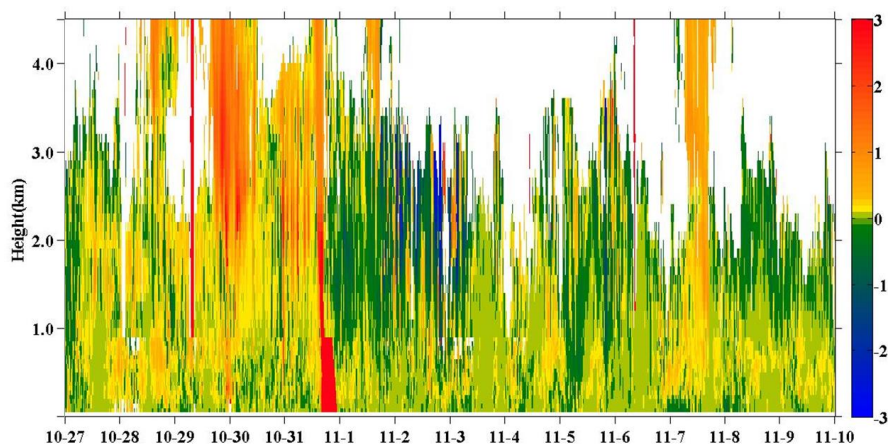


Figure 5. Vertical profile of wind vertical direction and speed (m/s, positive stands for up and negative stands for down) during the observation time at Liulihe site

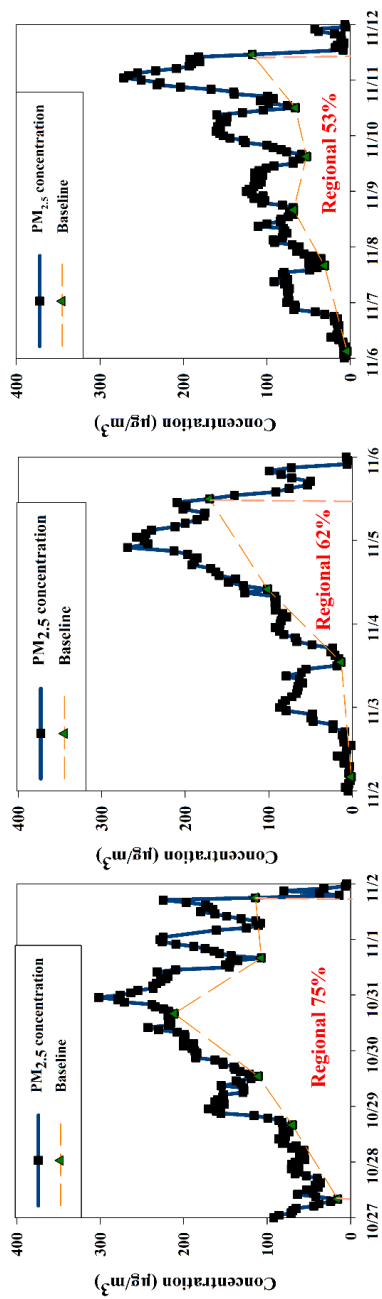


Figure 6. Regional and local components of the three episodes at Lulluhe site

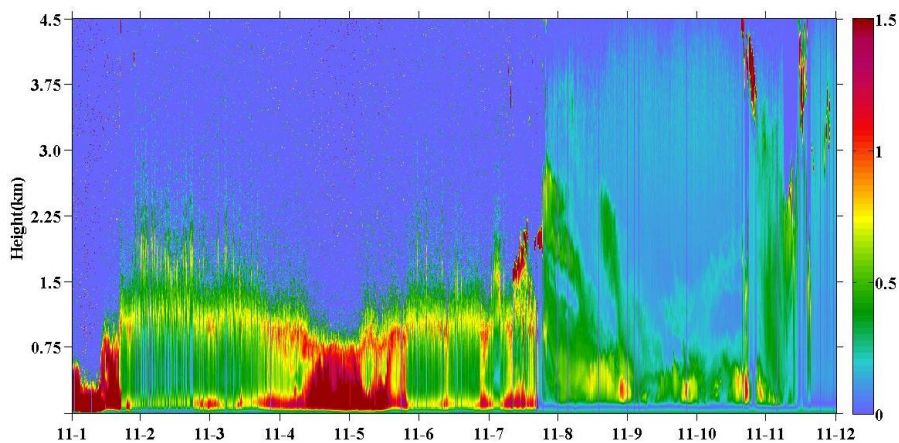


Figure 7. Vertical profile of extinction coefficient during the observation at Liulihe site

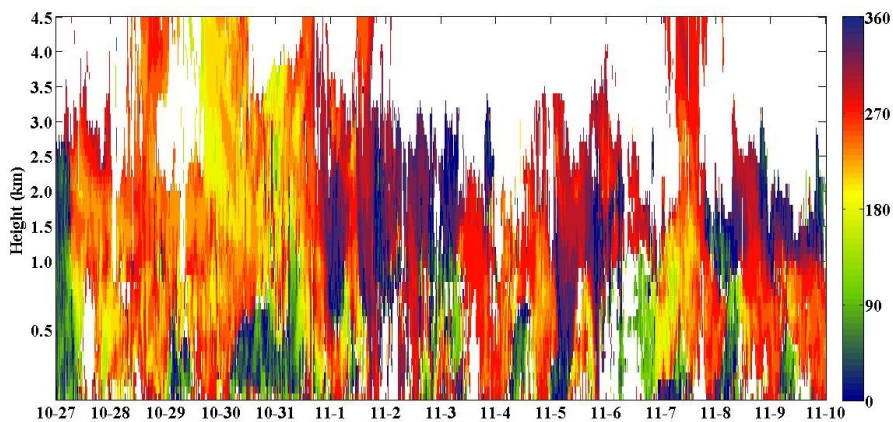
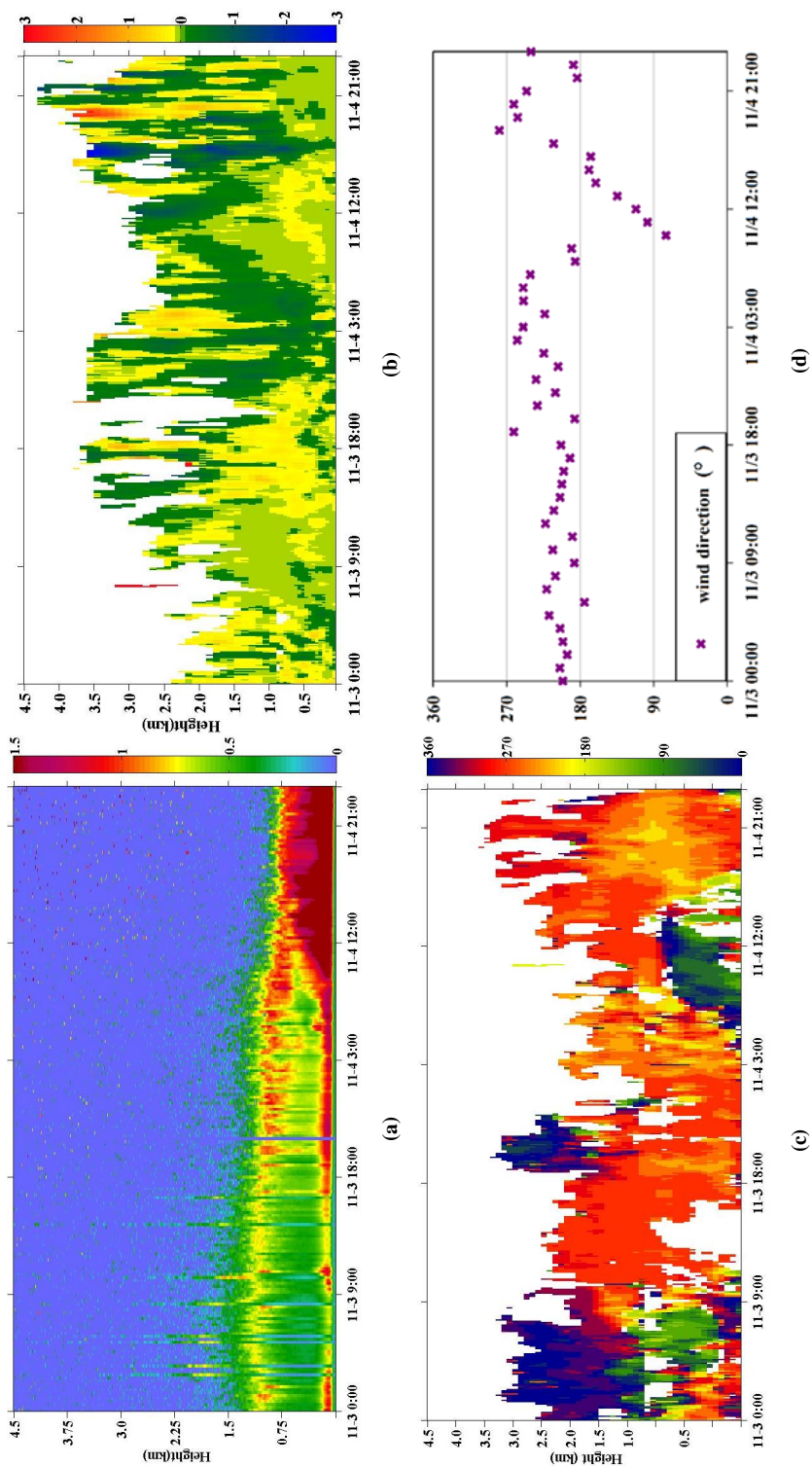


Figure 8. Vertical profile of wind horizontal direction during the observation at Liulihe site



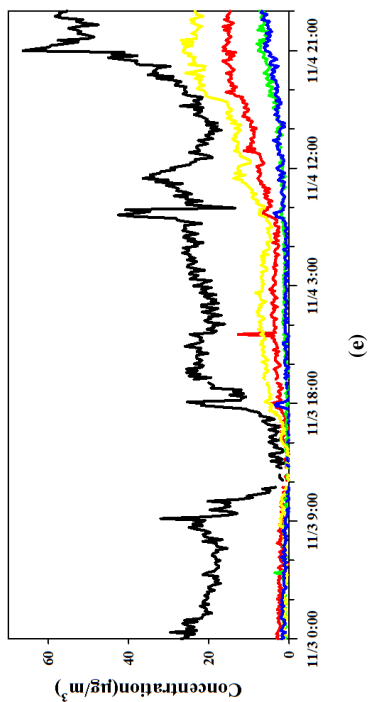
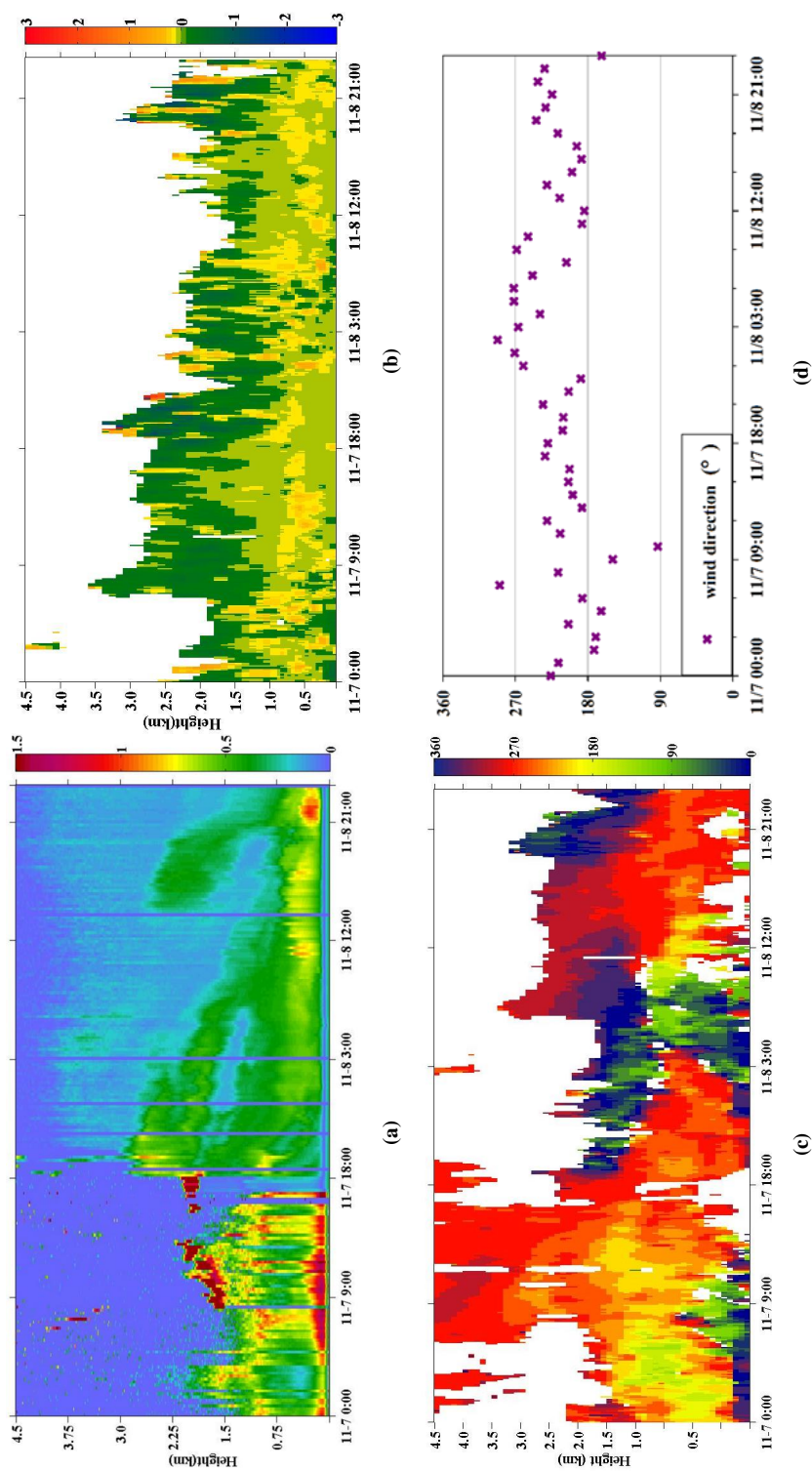
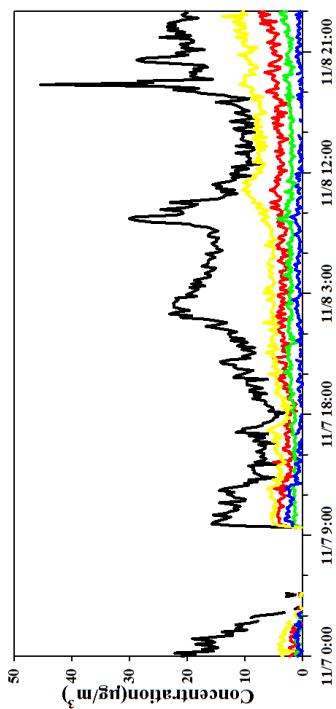


Figure 9. Parameters of particles and meteorology at Lulihe site during episode 2

(a) Vertical profile of extinction coefficient (km^{-1}); (b) Vertical profile of wind vertical direction and speed (m/s, positive stands for up, negative stands for down); (c) Horizontal wind direction profile ($^{\circ}$; 0° stands for north); (d) wind direction on the ground; (e) PM_{10} chemical components.





(e)

Figure 10. Parameters of particles and meteorology at Lulihe site during episode 3

(a) Vertical profile of extinction coefficient (km^{-1}); (b) Vertical profile of wind vertical direction and speed (m/s, positive stands for up, negative stands for down); (c) Horizontal wind direction profile ($^{\circ}$; 0° stands for north); (d) wind direction on the ground; (e) PM_{10} chemical components.

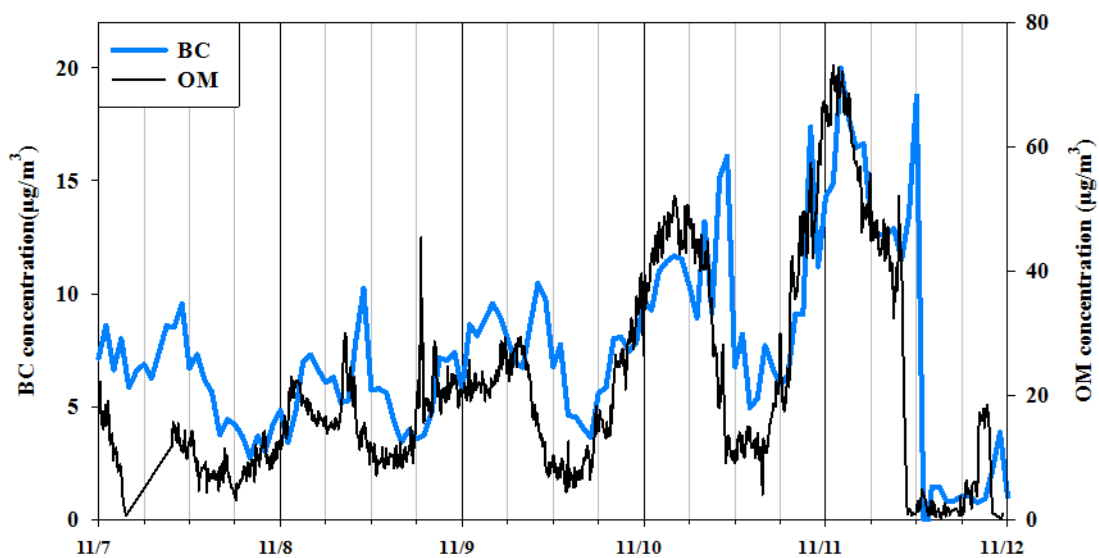


Figure 11. BC and OM concentrations of PM₁ at Liulihe site during episode 3